Influence of leaching on surface composition, microstructure and valence band of single grain icosahedral Al-Cu-Fe quasicrystal

M. Lowe,[1] T. P. Yadav,[2] V. Fournée,[3] J. Ledieu,[3] R. McGrath,[1] and H. R. Sharma[1]

[1)] *Surface Science Research Centre and The Department of Physics, The University of Liverpool, Liverpool, L69 3BX, UK*

[2)] *Hydrogen Energy Centre, Department of Physics, Banaras Hindu University, Varanasi, 221005, India*

[3)] *Institut Jean Lamour (UMR7198 CNRS-Université de Lorraine), Parc de Saurupt, 54011 Nancy Cedex, France*

(Dated: 28 April 2016)

The use of quasicrystals as precursors to catalysts for the steam reforming of methanol is potentially one of the most important applications of these new materials. To develop application as a technology requires a detailed understanding of the microscopic behavior of the catalyst. Here we report the effect of leaching treatments on the surface microstructure, chemical composition and valence band of the icosahedral (*i*-) Al-Cu-Fe quasicrystal in an attempt to prepare a model catalyst. The high symmetry fivefold surface of a single grain *i*-Al–Cu–Fe quasicrystal was leached with NaOH solution for varying times and the resulting surface was characterized by x-ray photoelectron spectroscopy (XPS), ultraviolet photoelectron spectroscopy (UPS), scanning electron microscopy (SEM) and atomic force microscopy (AFM). The leaching treatments preferentially remove Al producing a capping layer consisting of Fe and Cu oxides. The subsurface layer contains elemental Fe and Cu in addition to the oxides. The quasicrystalline bulk structure beneath remains unchanged. The subsurface gradually becomes Fe_3O_4 rich with increasing leaching time. The surface after leaching exhibits micron sized dodecahedral cavities due to preferential leaching along the fivefold axis. Nanoparticles of the transition metals and their oxides are precipitated on the surface after leaching. The size of the nanoparticles is estimated by high resolution transmission microscopy (TEM) to be 5-20 nm, which is in agreement with the AFM results. Selected area electron diffraction (SAED) confirms the crystalline nature of the nanoparticles. SAED further reveals the formation of an interface between the high atomic density lattice planes of nanoparticles and the quasicrystal. These results provide an important insight into the preparation of model catalysts of nanoparticles for steam reforming of methanol.

I. INTRODUCTION

Quasicrystals (QCs) have long-range ordered structures with no translational symmetry. They are intermetallic compounds (IMCs) with a specific chemical composition and possess classically forbidden rotational symmetries such as fivefold and tenfold. Quasicrystalline structure was first observed in 1982 during investigations of rapidly solidified Al-Mn alloys, which displayed icosahedral symmetry in the diffraction pattern[1]. QCs show physical properties that differ from those of structurally simple intermetallic compounds or amorphous alloys. These can include low coefficients of friction, high hardness, low surface energies, substantial wear resistance, low thermal and electrical conductivity. So far their use is restricted to niche applications[2–5].

A potentially attractive industrial application of QCs is in heterogeneous catalysis, specifically the steam reforming of methanol for hydrogen production[6–10]. Most quasicrystals contain catalytically active elements (for example, Pd, Cu, Fe, Ni), while also being brittle enough to facilitate high surface area through crushing. The steam reforming of methanol is being investigated for its benefits as a reaction for mobile hydrogen production for methanol fueled, hydrogen fuel cell powered vehicles[11]. Intermetallic compounds are also being investigated widely within the steam reforming of methanol and other hydrogenation reactions. IMCs provide the opportunity to use better suited materials to achieve the same catalytic behaviour as currently used materials. There is growing evidence to support the idea that being able to tune a materials electronic and atomic structure allows the material to have highly desirable results. With IMCs it has been possible to guarantee the dispersion of active sites by using an active species located regularly in a periodic lattice[12]. It has also been shown that IMCs can be chosen to mimic the electronic structure of good catalysts with excellent results[13].

Currently, Cu based catalysts are used industrially for the steam reforming of methanol but suffer from thermal instability and rapid degradation due to sintering of Cu particles which reduces the surface area of the catalyst[14]. In previous work performed by Tsai *et al.*, Al-based quasicrystals were found to show desired activity and stability for the reaction once powdered samples had been chemically treated in NaOH[6,9,10,15–18]. These materials also contain no precious metals and therefore are relatively cheap to manufacture. This leaching treatment was initially used to remove the passivating oxide layer arising from the surface Al, although the study showed the removal of Al metal from the quasicrystal also. When the Al-Cu-Fe quasicrystal was leached, all that remained in the surface region, as determined by x-ray diffraction (XRD), were Cu and Fe oxides in the form of nanoparti-

cles. These nanoparticles are believed to be responsible for the catalytic activity, whereby the Fe species act to disperse the active Cu species and inhibit sintering.

This type of leaching process is more commonly used in the production of Raney catalysts, and in the case of steam reforming of methanol, especially Raney Cu catalysts[19,20]. The leaching treatment in these materials allows the removal of Al species leaving behind a porous skeletal structure of Cu catalyst. Leached QCs have been shown to have a higher surface area, higher surface area of Cu and greater Cu dispersion across the surface[10]. In reaction studies leached QC catalysts have been found to produce more H_2 in comparable conditions. It is known that while sintering of Cu in Raney catalysts begins at even low reaction temperatures, Cu in QC catalysts has been shown to remain dispersed, and remarkably stable. This was attributed to either the dispersing presence of Fe or the interaction with the QC structure[10].

The Al-Cu-Fe approximants, which are periodic but have local structure and chemical composition similar to QCs, show less advantageous behaviour after treatment in comparison to the quasicrystal. A higher Al dissolution rate in the crystalline samples, because of homogeneous distribution of Al, produces layers of Cu species and not the desired dispersal of the active sites, leading to unfavorable activity[16].

The inherent complexity associated with quasicrystals combined with the limitations of surface science techniques on powdered samples have made the understanding of the changes associated with the surface difficult to determine. It was with this motivation that our experiment focused on recreating the treatments carried out by Tsai *et al.*, on simplified model systems. These model systems are single grain crystals with well oriented and well understood surfaces. Nanoparticles of the catalytically active metals are produced on the surface, through an adaptation of the leaching treatment. We have employed x-ray photoelectron spectroscopy (XPS) and ultraviolet photoelectron spectroscopy (UPS) to investigate the influence of leaching treatment on surface chemical composition and valence band structure of the fivefold surface of *i*-Al-Cu-Fe QC. The microstructure of the surface after leaching is also investigated by transmission electron microcopy (TEM), scanning electron microscopy (SEM) and atomic force microscopy (AFM). Selected area electron diffraction (SAED) is used to establish the epitaxial relationship between the nanoparticles and the underlying quasicrystal. The results presented below provide insight into the requirements for the preparation of model catalysts for the steam reforming of methanol.

II. EXPERIMENTAL PROCEDURE

A single grain sample of *i*-$Al_{63}Cu_{24}Fe_{13}$ was grown by the Bridgman method and cut along the fivefold surface. The orientation of the surface was confirmed through low energy electron diffraction (LEED), before leaching treatments were conducted. For LEED measurements, the surface was prepared as described in Ref.[21]. Before each leaching treatment, the surface was freshly polished with diamond paste of successively finer grades, from 6 to 0.25 µm. Leaching was performed by placing droplets of NaOH with 10 mol conc. (40% wt.) on the surface with a pipette, and maintaining the droplet against the process of evaporation. Leaching times of 1, 2, 4, 6, 8 hours were used to investigate the effect of leaching time on surface chemistry. After each leaching, the surface was thoroughly washed with methanol and distilled water in an ultrasonic bath.

Following chemical treatment, the crystal was placed in UHV (10^{-10} mbar) for XPS and UPS measurements. The sample was placed in the fast entry lock of the system and pumped down for 12-14 hours before being inserted into the analysis chamber.

Micro structure of the surface after leaching treatment was analyzed by SEM, AFM and TEM. The surface was freshly prepared (polished, leached and washed) before each microstructure analysis. TEM was carried out on a thin strip of the leached sample (10 μm thick) using a FEI-Tecnai 20 G2 electron microscope at 200 keV employing imaging and diffraction modes. The thickness of the leached area in the strip was less than 1 μm as estimated from the brightness of the transmitted beam.

The sample used for the TEM and SAED measurements was different from the one used for the other experiments. The sample was grown as described in Ref.[22]. The composition was *i*-$Al_{63}Cu_{25}Fe_{12}$, which was very close to the first sample. XRD confirmed the single icosahedral phase of the sample, as the case of the other sample. The sample consisted of multi-grains with grain size of 30-50 μm. The TEM results analyzed here were obtained from single grains. The sample was leached with the same method as before. Although the orientation of the surface was random in this sample, the sample could be adjusted in SAED experiments in order to probe the interface parallel to the fivefold surface. The SAED patterns presented in this report were obtained with a tilt angle of about 2° from the beam normal. Therefore, the surface orientation of the chosen grains was almost fivefold.

III. RESULTS AND DISCUSSION

This section is organized as follows. We first present different methods of surface preparation, particularity the effect of washing of the leached surface by water and methanol, in Section III A. The surface chemical composition of the leached surface investigated by XPS is discussed in Section III B and III C. The effect of leaching time on chemical composition is analyzed in Section III D. UPS results on the valence band structure of the leached surface is given in Section III E, while the structure of the leached surface characterized by SEM, AFM

	Al *2p*	Cu $2p_{3/2}$	Fe $2p_{3/2}$	O *1s*	C *1s*	Cu $L_3M_{45}M_{45}$
Elemental	72.8[23]	932.6	706.9[24]	531.0	284.9	918.6
Clean quasicrystal	72.9	933.8	707.0	n/a	n/a	918.1
Leached	n/a	932.7	711.0	530.2, 532.0	284.9	917.1
Leached + Sputtered	n/a	932.7	707.0, 710.0	530.4	n/a	918.6
Fe_3O_4	n/a	n/a	710.6[24]	530.1[24]	n/a	n/a
Fe_2O_3	n/a	n/a	711.0[24]	529.8[24]	n/a	n/a
Cu_2O	n/a	932.5[25]	n/a	530.5[25]	n/a	916.5[26]
CuO	n/a	933.8[25]	n/a	529.6[25]	n/a	917.8[26]

TABLE I. Binding energies (eV) of Al, Cu, and Fe core levels in various forms: elemental, oxides, clean *i*-Al-Cu-Fe quasicrystal, quasicrystal after leaching treatment (2 hours) and subsequent sputtering. The last column presents kinetic energies of the Cu LMM Auger transition. Data taken from the literature[23–26] are referenced. The rest of the data are from this work.

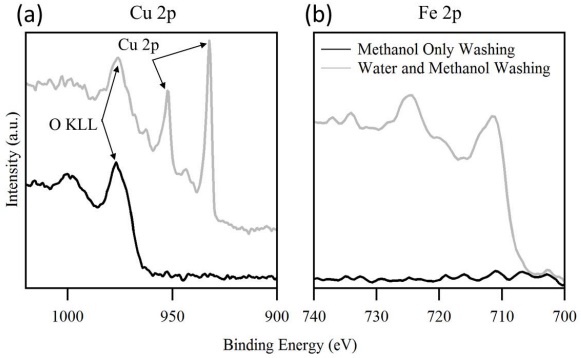

FIG. 1. (a) Cu *2p* and (b) Fe *2p* XPS spectra (Al K_α source) from the fivefold *i*-Al-Cu-Fe surface after leaching (1 hour), followed by water and methanol, and methanol-only washing procedures.

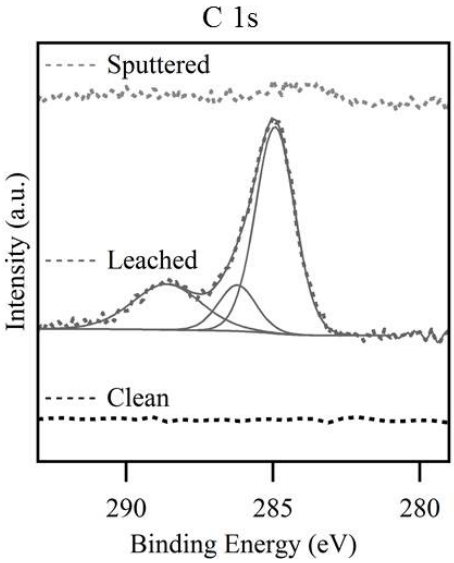

FIG. 2. C *1s* XPS peak (Mg K_α source) from the surface after leaching (2 hours) and subsequent sputtering in UHV. A spectrum of the clean quasicrystal surface prepared in UHV is also given for comparison. Solid curves correspond to the results of a fit as described in the text.

and TEM is presented in Section III F. Finally, the interfacial relationship between the leached surface and the bulk studied by SAED is discussed in Section III G.

A. The Effect of Post-Leaching Treatments

Sonic cleaning using methanol is a standard procedure for UHV experiments. However, we were unable to remove species related to the remains of the leaching solution from the surface by this method. XPS from the surface cleaned with methanol showed a shift in the Na 1s core level binding energy, and many features in the O and C 1s peaks. This indicates the presence of salts and oxides as a result of the leaching solution. The XPS spectra were completely dominated by the peaks associated with the Na core levels, plus large O and C peaks such that the core levels of the expected quasicrystal components were not visible (Figure 1). The NaOH solution was dissolved after washing with deionized water. This then allowed the use of methanol cleaning, in line with usual UHV/surface science methods.

The surface after leaching, followed by washing with water, yielded an XPS spectrum exhibiting the core level peaks of the constituents of the quasicrystal. However, the surface was still heavily contaminated from being exposed to air before insertion into UHV. This led to scans lacking in intensity and diffuse peaks. Sputtering the surface using 2 keV Ar^+ for 30-40 min removed the physisorbed species of both C *1s* and O *1s* (Figure 2), improving the resolution of the peaks. The O *1s* core levels will be discussed in Section III B. As shown in Figure 2, the C 1*s* peak could be fitted with three components corresponding to the C 1*s* core levels of C-C, C-O and C=O compounds[27]. All of these peaks are removed by sputtering.

Once the sample is sputtered, the surface no longer resembles the surface that would take part in the reaction. As such, strong conclusions regarding the catalytic activity of the sputtered surface should be avoided. The sput-

tering process does however, provide the opportunity to study the subsurface region, and potentially the interface between the QC and resulting species above. The cleaning process (washing with water followed by methanol) was the same for all of the experiments.

B. Effect of Leaching on Surface Chemical Composition

The surface chemical composition after different surface treatments was determined by analyzing the XPS spectra. XPS spectra from the clean (sputter-annealed), leached and leached-sputtered surfaces are compared in Figure 3. The core level binding energies of the species after each treatment are presented in Table I and compared with those from pure metals and their oxides. The core level binding energies were analyzed by fitting the peaks using a Gaussian-Lorentzian curve and Shirley background subtraction. An example of such a fit is given in Figure 2. The uncertainty in the given core level binding energies is estimated to be 0.1-0.2 eV. Each of the core levels of each species is discussed below.

Removal of Al from the Surface

As shown in Figure 3 (a), the Al *2p* peak of the clean surface disappears after leaching. The Cu and Fe core levels are still detected. This confirms the selective dissolution of Al from the surface. XPS spectra shown in Figure 3 were taken after 2 hours leaching. Other data show that the Al *2p* peak of the clean surface is already removed after 1 hour leaching. Longer exposure to the leaching solution modifies the composition of the Cu and Fe species in the surface, which will be discussed in Section III D. The Al core levels of the clean surface were not detected even after sputtering, indicating the absence of Al in the subsurface region too. Although no Al of the clean surface was observed, a trace of aluminium oxide is detected. This was evidenced by a shift of the Al *2s* peak to a higher energy (not shown). The Al *2p* peak of the oxide overlaps with the Cu *3p* peaks and thus it is difficult to identify the oxide contribution by analyzing the Al *2p* peak. A trace of Al oxide was detected even after the surface was sputtered.

Identification of Cu Species

The Cu core levels are shifted to a lower binding energy after leaching (Figure 3 (a) and (c)). The Cu $2p_{3/2}$ is shifted to 932.7 eV, which is close to the binding energy of elemental Cu or Cu_2O. The Cu *2p* core level in elemental Cu and in Cu_2O is separated only by 0.4 eV[28]. Thus, it is difficult to distinguish the two species by XPS with the given experimental resolution. However, they can be distinguished by comparing the Cu Auger transition peak, as the Cu LMM Auger peaks of the two species are separated by about 2 eV[26].

The Cu LMM Auger peak from the leached surface is observed at 917.1 eV kinetic energy (Figure (3)d), which is close to the Cu LMM transition for Cu_2O or CuO[26]. However, we rule out the formation of CuO based on the observed Cu core levels. The Cu *2p* for CuO is expected to be shifted to higher binding energy by 1.2 eV with respect to elemental Cu but no shift is expected for Cu_2O. We did not observe a shift in Cu *2p*, confirming the absence of CuO. After sputtering, only a trace of Cu_2O is detectable and a new peak appears at 918.6 eV, which is the characteristic energy of elemental Cu. This suggests the presence of elemental Cu in the subsurface region.

Identification of Fe Species

An XPS spectrum from the clean *i*-Al-Cu-Fe surface shows the Fe $2p_{3/2}$ peak at 707.0 eV (Figure 3 (b)). The peak appears at almost the same binding energy as elemental Fe[24]. The Fe $2p_{3/2}$ peak is shifted to higher binding energy after leaching, which is attributed to the formation of Fe oxides. After sputtering, an additional peak emerges, as in the case of the Cu species discussed above. This new peak appears at the same position as elemental Fe, or Fe in the *i*-Al-Cu-Fe QC. Since no other evidence of the underlying quasicrystal can be identified by XPS following leaching and even after sputtering, we conclude that this peak must be due to elemental Fe, and not from the quasicrystal. If the bulk is probed, Al, the dominant constituent, should also be detected. But Al was not detected after sputtering as discussed above.

Because of peak broadness, it is not possible to precisely determine the position of the Fe $2p$ peak of the oxide. However, it is clear that after sputtering the Fe $2p_{3/2}$ peak is shifted to a lower binding energy by about 1 eV. This shift can be explained if the top layers are predominantly Fe_2O_3 and the subsurface contains Fe_3O_4. The Fe $2p$ peak of Fe_2O_3 is expected to appear at higher binding energy than Fe_3O_4 (Table 1). Sputtering removes the top layers of Fe_2O_3 and thus exposes the subsurface Fe_3O_4. We cross-checked the existence of both oxides by analyzing the O *1s* core level, which we describe below.

Analysis of O Core Levels

Fitting the O $1s$ peak is challenging because of the presence of multiple oxides and hydroxides. Nevertheless, the O *1s* peak after leaching can be fitted by five components (Figure 4). By comparing the peak positions with XPS results from Fe nanoparticles dispersed on a glass substrate[29], we suggest that peaks 1 and 4 are due to Fe_2O_3 and water, respectively. Peak 3 is related to hydroxide and/or defects in the Fe_2O_3 lattice[29]. Peak 2 is contributed by Cu_2O[25]. The binding energy of peak 5, which is weaker in intensity, is close to the O $1s$ core

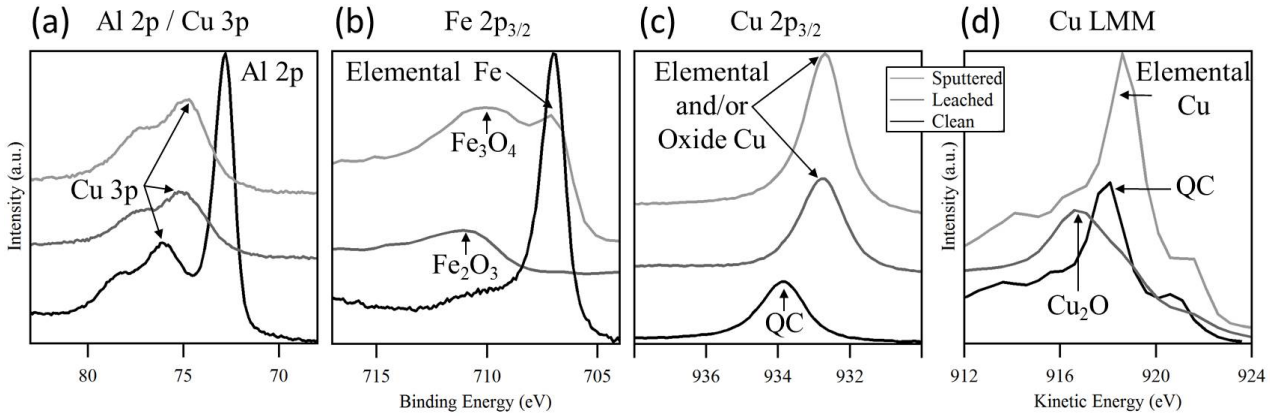

FIG. 3. (a) Al *2p*/Cu *3p*, (b) Fe *2p*, (c) Cu *2p*, and (d) Cu LMM spectra (Mg K_α source) from the fivefold *i*-Al-Cu-Fe surface after leaching (2 hours) and subsequent sputtering. Results from the clean surface are also given for comparison.

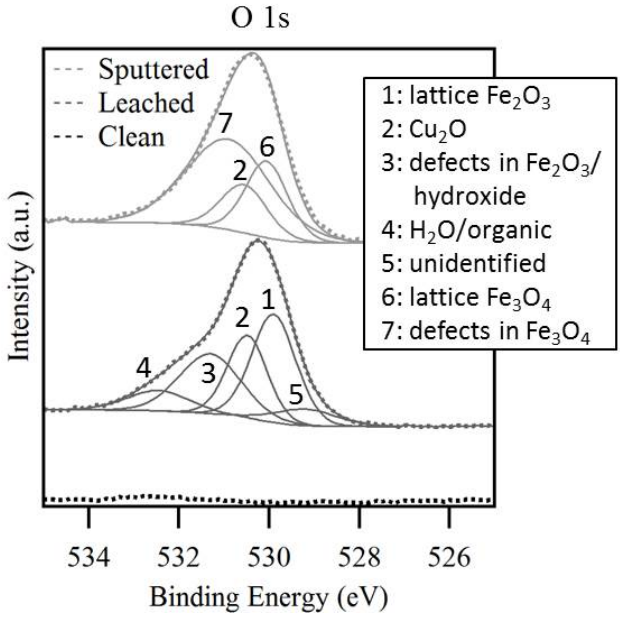

FIG. 4. O *1s* XPS core level (Mg K_α source) from the surface after leaching (2 hours) and subsequent sputtering in UHV. The spectrum from the clean quasicrystal surface prepared in UHV is also given for a comparison. Solid curves correspond to the results of a fit as described in the text.

level of FeO[30]. However, it is difficult to confirm the existence of FeO by analyzing the Fe core levels because of low peak intensity. After sputtering, the water and hydro-oxide peaks are removed. Nevertheless, a contribution from Cu_2O is still detectable, in agreement with the Auger result discussed above. The O 1*s* peak after sputtering can be fitted with only three components: O 1*s* of Cu_2O, Fe_3O_4 and defective oxygen sites of Fe_3O_4[29].

C. Layered Structure Formed by Leaching

Based on the surface chemical composition analyzed above, we propose a model structure of the surface yielded by leaching and subsequently washing with water. The surface consists of layers of different compositions. The top layers contain Fe_2O_3 and Cu_2O, while the subsurface layer contains elemental Cu, Fe, Fe_3O_4 and a trace of Cu_2O. Fe_2O_3 is expected to form an overlayer in Fe-based compounds upon oxidation[24]. We affirm the formation of the layered structure based on the fact that only the oxide species were observed before the surface was sputtered, while the elemental species emerged only after sputtering. Our hypothesis is that the top oxide layers are removed by sputtering, exposing subsurface layers to be detected by XPS. Fe_2O_3 is not observed after sputtering and Cu_2O is significantly reduced. This indicates the absence of Fe_2O_3 and only a trace of Cu_2O in the subsurface region.

After the leaching experiments, the surface was polished and prepared in UHV by sputtering and annealing, and was examined by LEED and STM. The surface exhibited quasicrystalline LEED patterns characteristic of the clean surface. Similarly, STM yielded atomic resolution characteristic of the original surface. This indicates that leaching occurs only in a limited depth from the surface. This is expected from the previous leaching experiments of powder samples. The cross-sectional TEM study showed that the dissolution of Al is restricted to a certain thickness (about a half of μm in the given experiment)[16] because of the inhomogeneous distribution of Al inherent to the quasicrystallinity of the sample studied. We also find the thickness of the leached area is less than 1 μm as described in Section II.

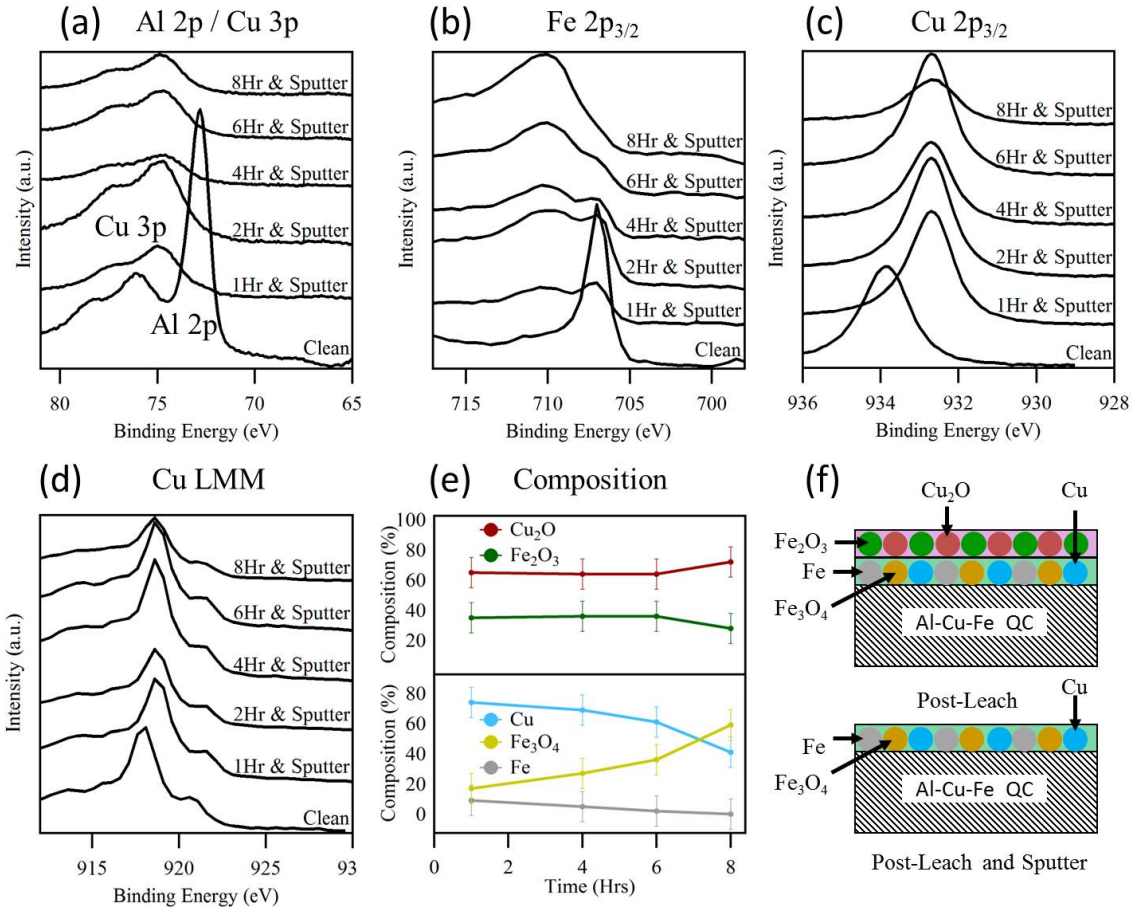

FIG. 5. (a) Al *2p*/Cu *3p*, (b) Fe *2p*, (c) Cu *2p*, and (d) Cu LMM Auger spectra (Mg K_α source) from the fivefold *i*-Al-Cu-Fe surface after leaching for different times and subsequent sputtering. (e) Change in composition of the top surface layers (top) and subsurface (bottom). The composition of the subsurface was deduced from XPS spectra given in (b) and (c). (f) Illustration of the surface and subsurface composition after leaching and sputtering.

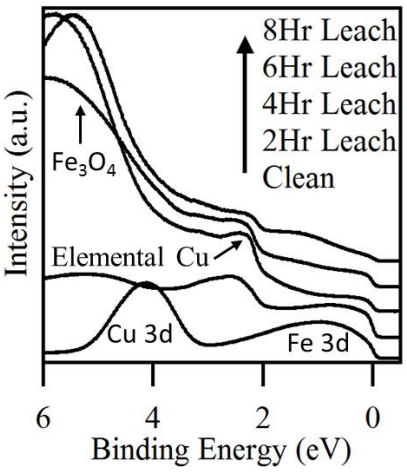

FIG. 6. Valence band spectra of the fivefold *i*-Al-Cu-Fe surface after leaching for different times taken with He-I radiation. The angle of incidence was 45°.

D. Effect of Leaching Time on Chemical Composition

XPS spectra from the surface after leaching at different times from 1 to 8 hours are compared in Figure 5 (a-d). The spectra were taken after the surface was sputtered and thus provide information from the subsurface region of the leached surface. The core level positions of Cu and Fe are not affected by increasing the leaching time. However, there is a change in surface chemical composition. The variation in the composition deduced from the XPS spectra for different leaching times is shown in Figure 5 (e), bottom. The composition was determined using the area of the Cu *2p* and Fe *2p* peaks after Shirley background subtraction and using the photoemission cross section, instrumental response and inelastic mean path of photoelectrons.

The content of Fe_3O_4 increases with leaching time, while elemental Fe and Cu decreases. After 6 hours we can no longer identify Fe metal, which was possible after shorter treatments. Elemental Cu is still detectable even after 8 hours leaching. This may be because the

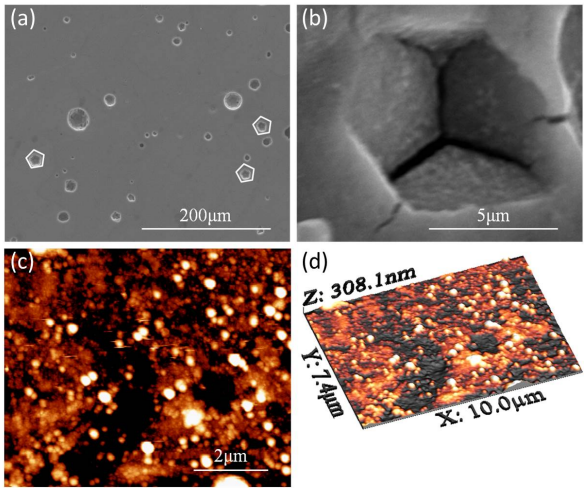

FIG. 7. (a) SEM image of the fivefold *i*-Al-Cu-Fe surface after leaching at 8 hours showing fivefold cavities across the surface (30 kV beam energy). (b) Dodecahedral cavity observed on the surface after leaching at 8 hours (30 kV beam energy) (c-d) AFM images of precipitate nanoparticles on the surface visualized in both 2D and 3D (leaching time 8 hours). AFM images were obtained in ambient conditions, not in UHV.

subsurface Fe gradually oxidizes with leaching time and becomes rich in Fe_3O_4. After 8 hours of leaching the surface is predominantly Fe_3O_4.

The change in composition in the surface region was also analyzed using XPS spectra from the leached surface, i.e., without sputtering. In contrast to the subsurface region, the Cu species increases and Fe species in the surface region decreases with increasing leaching, especially after 6 hours leaching (Figure 5 (e), top). The influence of leaching time has not been systematically studied on the powder samples. However, the powder sample leached by 5 mol concentration of NaOH for 12 hours exhibited the Cu species[6,9] and there are no reports of identification of elemental Fe.

E. Effect of Leaching on Valence Band

UPS measurements were performed from the surface after leaching for different times and subsequently sputtering in UHV (Figure 6). The valence band spectrum from the clean quasicrystal surface shows two peaks corresponding to the Cu *3d* band (at about 4 eV) and the Fe *3d* band near to the Fermi level[31]. After leaching for 2 hours, three peaks appeared in the valence band. The peak at about 5 eV is attributed to Fe_3O_4[32], the peak at around 2.5 eV to elemental Cu[33] and the peak near to the Fermi level to elemental Fe[32]. With increasing leaching time, the spectra demonstrate the increase in the Fe_3O_4 intensity and the gradual removal of elemental Cu and Fe peaks, in agreement with the XPS results discussed above.

F. Microstructure of the Leached Surface

The microstructure of the surface was characterized by SEM, AFM and TEM. SEM revealed that after leaching the surface develops micron sized pentagonal holes with predominantly identical orientation (Figure 7 (a-b)). Longer exposure to the leaching solution yields dodecahedral cavities. The formation of the dodecahedral cavities can be explained if the surface is preferentially leached along all fivefold planes, and not limited to the fivefold plane parallel to the surface[34]. We recall that the icosahedral quasicrystal has six fivefold axes inclined at 63.4° from each other. Further detail of the surface microstructure at different leaching times has been described previously[34].

A closer look at the surface after leaching reveals the presence of nanoparticles on the surface. In our previous report, we were unable to image the surface with sufficient magnification to successfully resolve the nanoparticles. In this study, we use TEM and AFM to get information on particle size. AFM images reveal the porous nature of the surface after leaching (Figure 7 (c-d)), in agreement with high resolution SEM. The root mean square roughness of the surface estimated from the 10 μm $\times$ 10 μm AFM image is about 30 nm, although in some places the roughness is much larger. Particles of two different sizes can be identified in AFM; the brighter features have larger lateral size than the grey features. The small particles are predominant. The size of the large particles is up to about 200 nm. The small particles are of approximately 20 nm size, which is comparable to the particle size observed on the leached powder by Tsai *et al*[6]. This size is also in good agreement with our TEM results, which are discussed below.

Figure 8 (a) shows a representative TEM microstructure of a thin strip of the sample after leaching at 8 hours, where the leached and un-leached areas are marked by 'B' and 'A', respectively. Nanosize particles are observed in the leached area, which are clearer in the high magnification image given in Figure 8 (b). The particle size was found to be 5-20 nm, which agrees well with the AFM results and powder samples[6].

G. Interface between nano particles and quasicrystal

The interfacial relation between the nanoparticles and the underlying quasicrystal was determined by comparing SAED patterns from the leached and un-leached areas. SAED patterns recorded by scanning the electron beam across the co-existing leached and un-leached areas are shown in Figure 8 (c, d). As expected, the un-leached region yields patterns characteristic of the icosahedral quasicrystal. However, the leached area produces rings, instead of spots, (Figure 8 (d)). The ring patterns suggest that the leaching treatment yields nano-grain microstructures aligned randomly on the quasicrystal interface.

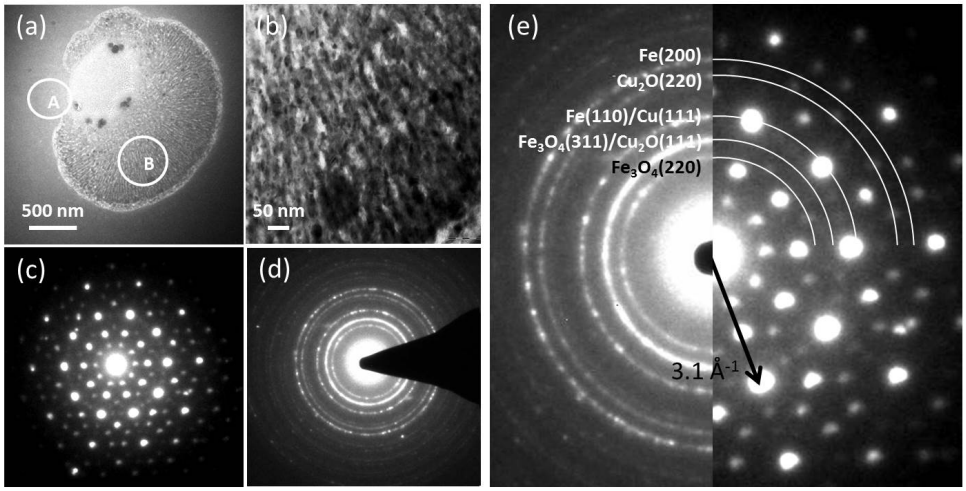

FIG. 8. (a) Bright field microstructure of the *i*-Al-Cu-Fe quasicrystal after leaching for 8 hours. 'A' and 'B' mark the un-leached and leached areas, respectively. (b) Highly magnified image of the leach region 'B'. (c-d) Selected area electron diffraction (SAED) patterns from region 'A' (c) and 'B' (d). (e) Comparison of SAED patterns from the leached and un-leached area.

The reciprocal lattice vectors (k-vectors) of the rings are consistent with those for elemental Cu and Fe, Cu_2O and Fe_3O_4. The rings are indexed in Figure 8 (e). We also find that the k-vectors of some of the rings match with those of the quasicrystal. The strongest diffraction spots from the quasicrystal, at 3.1 $Å^{-1}$ (= k_0), coincide with the Cu(111) and Fe(110) rings with a mismatch of only 2-3%, which is within the experimental uncertainty. The matching of the k-vectors suggest the formation of an interface between the fivefold surface and high atomic density planes of Cu(111), Fe(110) and Fe(200). This is in agreement with the conclusion drawn from the XPS results that the subsurface region after leaching is richer in elemental Cu and Fe than the oxide. Cu(111) and Fe(110) are the highest atomic density planes, Cu and Fe having fcc and bcc structure, respectively. Fe(200) has the second highest atomic density in the Fe bcc structure. Similarly, the fivefold surface of the *i*-Al-Cu-Fe QC terminates at high density planes of the bulk structure. This suggests that the interface is formed between the high density planes of nano-particles and the quasicrystal. We recall that the *i*-Al-Cu-Fe quasicrystal powder shows higher thermal stability than metal catalysts in steam reforming of methanol[6]. We suggest that the interface between high density planes may provide this higher stability.

IV. CONCLUSIONS

We have studied the effect of leaching treatments on the microstructure, chemical composition and valence band of the *i*-Al–Cu–Fe quasicrystal. The fivefold surface of the single grain *i*-Al–Cu–Fe sample was leached with NaOH solution for varying times and the resulting surfaces were characterized by XPS, UPS, SEM, AFM, TEM and SAED. The leaching treatments preferentially remove Al, producing a capping layer of Fe and Cu oxides. The subsurface layer contains the transition metal species in addition to the oxides, while the quasicrystal structure beneath remains unchanged. The surface gradually becomes rich in Fe_3O_4 with increasing leaching time. The leached surface displays facets and cavities exhibiting fivefold symmetry and a common orientation. This is explained by preferential leaching along the fivefold axes. The surface after leaching is porous and contains nanoparticles. The size of the particles is 5-20 nm as confirmed by AFM and TEM. SAED confirms the formation of nanoparticles of Cu, Fe, Cu_2O and Fe_3O_4. The interface is formed between high atomic density lattice planes of the nano particles and the quasicrystal. The formation of such an interface may provide a greater stability to the nanoparticles during catalytic reactions.

ACKNOWLEDGMENTS

This work was supported by the Engineering and Physical Sciences Research Council (grant number EP/D071828/1). The authors are grateful to R. Clowes and A. I. Cooper for the use of high resolution SEM within the University of Liverpool Centre for Materials Discovery. The authors would also like to thank A. P. Tsai from Tohoku University for helpful discussions. The authors also thank D. Martin from the University of Liverpool for providing access to AFM and P. Unsworth and P. Weightman for assisting in preliminary XPS measurements. ML would like to acknowledge EPSRC for a doctoral training grant, and the European Integrated Centre for the Development of New Metallic Alloys and

Compounds (C-MAC) for scientific exchange funding.

[1] D. Shechtman, I. Blech, D. Gratias, and J. W. Cahn, "Metallic Phase with Long-Range Orientational Order and No Translational Symmetry," Physics Review Letters **53**, 1951–1953 (1984).

[2] Z. Stadnik, *Physical Properties of Quasicrystals*, Springer Series in Solid State Sciences, Vol. 126 (Springer, Berlin, 1999).

[3] J.-M. Dubois, "So Useful, Those Quasicrystals," Israel Journal of Chemistry **51**, 1168–1175 (2011).

[4] J.-M. Dubois, "Properties- and Applications of Quasicrystals and Complex Metallic Alloys," Chem. Soc. Rev. **41**, 6760–6777 (2012).

[5] S. Kenzari, D. Bonina, J. M. Dubois, and V. Fournée, "Complex Metallic Alloys as New Materials for Additive Manufacturing," Sci. Technol. Adv. Mater. **15**, 024802 (2014).

[6] A. P. Tsai and M. Yoshimura, "Highly Active Quasicrystalline Al-Cu-Fe Catalyst for Steam Reforming of Methanol," Applied Catalysis A-General **214**, 237–241 (2001).

[7] M. Yoshimura and A. P. Tsai, "Quasicrystal Application on Catalyst," Journal of Alloys and Compounds **342**, 451–454 (2002).

[8] B. P. Ngoc, C. Geantet, M. Aouine, G. Bergeret, S. Raffy, and S. Marlin, "Quasicrystal Derived Catalyst for Steam Reforming of Methanol," International Journal of Hydrogen Energy **33**, 1000–1007 (2008).

[9] S. Kameoka, T. Tanabe, and A. Tsai, "Al-Cu-Fe Quasicrystals for Steam Reforming of Methanol: A New Form of Copper Catalysts," Catalysis Today **93-95**, 23–26 (2004).

[10] T. Tanabe, S. Kameoka, and A. Tsai, "A Novel Catalyst Fabricated from Al-Cu-Fe Quasicrystal for Steam Reforming of Methanol," Catalysis Today **111**, 153–157 (2006).

[11] J. C. Amphlett, K. A. M. Creber, J. M. Davis, B. A. Peppley, and D. M. Stokes, "Hydrogen Production by Steam Reforming of Methanol for Polymer Electrolyte Fuel Cells," Internation Journal of Hydrogen Energy **19**, 131–137 (1994).

[12] M. Armbruster, K. Kovnir, M. Friedrich, D. Teschner, G. Wowsnick, M. Hahne, P. Gille, L. Szentmiklosi, M. Feuerbacher, M. Heggen, F. Girgsdies, D. Rosenthal, R. Schlogl, and Y. Grin, "$Al_{13}Fe_4$ as a low-cost alternative for palladium in heterogeneous hydrogenation," Nat Mater **11**, 690–693 (2012).

[13] A. P. Tsai, S. Kameoka, and Y. Ishii, "Pdzn=cu: Can an intermetallic compound replace an element?" Journal of the Physical Society of Japan **73**, 3270–3273 (2004), http://dx.doi.org/10.1143/JPSJ.73.3270.

[14] D. R. Palo, R. A. Dagle, and J. D. Holladay, "Methanol Steam Reforming for Hydrogen Production," Chemical Reviews **107**, 3992–4021 (2007).

[15] A. Tsai and M. Yoshimura, "Quasicrystalline Catalyst for Steam Reforming of Methanol," Materials Research Society Symposium Proceedings **643**, K16.4.1–9 (2001).

[16] T. Tanabe, S. Kameoka, and A. P. Tsai, "Microstructure of Leached Al-Cu-Fe Quasicrystal with High Catalytic Performance for Steam Reforming of Methanol," Applied Catalysis A: General **384**, 241–251 (2010).

[17] T. Tanabe, S. Kameoka, E. Sato, M. Terauchi, and A. P. Tsai, "Cross-Section TEM Investigation of Quasicrystalline Catalysts Prepared by Aqueous NaOH Leaching," Philosophical Magazine **87**, 3103–3108 (2007).

[18] T. Tanabe, S. Kameoka, and A. P. Tsai, "Evolution of Microstructure Induced by Calcination in Leached Al-Cu-Fe Quasicrystal and its Effects on Catalytic Activity," Journal of Materials Science **46**, 2242–2250 (2011).

[19] M. Raney, "Method of preparing catalytic material," (1925).

[20] A. A. Pavlic and H. Adkins, "Preparation of a raney nickel catalyst," Journal of the American Chemical Society **68**, 1471–1471 (1946), http://dx.doi.org/10.1021/ja01212a023.

[21] H. R. Sharma, V. Fournée, M. Shimoda, A. R. Ross, T. A. Lograsso, A. P. Tsai, and A. Yamamoto, "Structure of the Fivefold Surface of the Icosahedral Al-Cu-Fe Quasicrystal: Experimental Evidence of Bulk Truncations at Larger Inter-Layer Spacings," Physical Review Letters **93**, 165502–165505 (2004).

[22] T. P. Yadav, S. S. Mishra, M. Lowe, R. Tamura, N. K. Mukhopadhyay, O. N. Srivastava, R. McGrath, and H. R. Sharma, "Leaching of Al-based Polygrain Quasicrystalline and Related Crystalline Surfaces," Acta Physica Polonica A **126**, 629–632 (2014).

[23] C. Hinnen, D. Imbert, J. M. Siffre, and P. Marcus, "An in situ XPS Study of Sputter-Deposited Aluminium Thin Films on Graphite," Applied Surface Science **78**, 219–231 (1994).

[24] N. S. McIntyre and D. G. Zetaruk, "X-ray Photoelectron Spectroscopic Studies of Iron Oxides," Analytical Chemistry **49**, 1521 (1977).

[25] N. S. McIntyre and M. G. Cook, "X-ray Photoelectron Studies on Some Oxides and Hydroxides of Cobalt, Nickel, and Copper," Analytical Chemistry **47**, 2208 (1975).

[26] J. P. Tobin, W. Hirshwald, and J. Cunningham, "XPS and XAES Studies of Transient Enhancement of Cu at CuO Surfaces During Vacuum Outgassing," Applications of Surface Science **16**, 441–452 (1983).

[27] J. Lu, Y. Lei, K. C. Lau, X. Luo, P. Du, J. Wen, R. S. Assary, U. Das, D. J. Miller, J. W. Elam, H. M. Albishri, D. A. El-Hady, Y.-K. Sun, L. A. Curtiss, and K. Amine, "A Nanostructured Cathode Architecture for Low Charge Overpotential in Lithium-Oxygen Batteries," Nature Communications **4**, 2383 (2013).

[28] S. Poulston, P. M. Parlett, P. Stone, and M. Bowker, "Surface Oxidation and Reduction of CuO and Cu_2O Studied Using XPS and XAES," Surface and Interface Analysis **24**, 811–820 (1996).

[29] M. C. Biesinger, B. P. Payne, A. P. Grosvenor, L. W. M. Lau, A. R. Gerson, and R. S. C. Smart, "Resolving Surface Chemical States in XPS Analysis of First Row Transition Metals, Oxides and Hydroxides: Cr, Mn, Fe, Co and Ni," Applied Surface Science **257**, 2717 (2011).

[30] V. Zabarskas, S. Tamulevičius, I. Prosyčevas, and J. Puišo, "Analysis of Fe_3O_4 Protective Coatings Thermally Grown on Color Picture TV Tube Structural Steel Components," Materials Science (Medžiagotyra) **10**, 147–151 (2004).

[31] J. A. Barrow, V. Fournée, A. R. Ross, P. A. Thiel, M. Shimoda, and A. P. Tsai, "Photoemission Studies of the Sputter-Induced Phase Transformation on the Al-Cu-Fe Surface," Surface Science **539**, 54–62 (2003).

[32] C. F. Brucker and T. N. Rhodin, "Oxygen Chemisorption and Reaction on α-Fe(100) Using Photoemission and Low-Energy Electron Diffraction," Surface Science **57**, 523–539 (1976).

[33] K. H. Schulz and D. T. Cox, "Photoemission and Low-Energy-Electron-Diffraction Study of Clean and Oxygen-Dosed Cu_2O (111) and (100) Surfaces," Physical Review B **43**, 1610–1621 (1991).

[34] T. P. Yadav, M. Lowe, R. Tamura, R. McGrath, and H. Sharma, "Effect of Leaching on Surface Microstructure and Chemical Composition of Al-Based Quasicrystals," in *Aperiodic Crystals*, edited by S. Schmid, R. L. Withers, and R. Lifshitz (Springer, Netherlands, 2013) Chap. 37, pp. 275–282.